

# PSD: Parallel finite element Solver for continuum Dynamics

Mohd Afeef Badri<sup>1</sup>, Giuseppe Rastello<sup>2</sup>, and Evelyne Foerster<sup>3</sup>

<sup>1</sup> Université Paris-Saclay, CEA, Service de Génie Logiciel pour la Simulation (SGLS), 91191, Gif-sur-Yvette, France <sup>2</sup> Université Paris-Saclay, CEA, Service d'Études Mécaniques et Thermiques (SEMT), 91191, Gif-sur-Yvette, France <sup>3</sup> Université Paris-Saclay, CEA, Département de Modélisation des Systèmes et Structures (DM2S), 91191, Gif-sur-Yvette, France ¶ Corresponding author

DOI: [10.xxxxxx/draft](https://doi.org/10.xxxxxx/draft)

## Software

- [Review](#)
- [Repository](#)
- [Archive](#)

Editor: ¶

Submitted: 07 October 2025

Published: unpublished

## License

Authors of papers retain copyright and release the work under a Creative Commons Attribution 4.0 International License ([CC BY 4.0](https://creativecommons.org/licenses/by/4.0/)).

## Summary

PSD (Parallel finite element Solver for continuum Dynamics) is an open-source finite element solver designed for high-performance computing simulations in continuum dynamics with a special focus on earthquake mechanics and structural dynamics. PSD addresses the computational challenges of large-scale seismic simulations by providing an integrated platform for analyzing complex dynamics problems in both two and three dimensions.

Built upon FreeFEM ([Hecht, 2012](#)) for finite element discretization and PETSc ([Balay et al., 2019](#)) for scalable linear system solving, PSD integrates sophisticated material modeling through its dedicated Mfront ([Helfer et al., 2015](#)), ([Helfer et al., 2020](#)) interface. This architecture enables the handling of complex material behaviors thanks to non-linear constitutive laws essential for realistic mechanical phenomena modeling. PSD includes a purpose-built MPI I/O-based mesher-partitioner, top-ii-vol ([Badri et al., 2024](#)), tailored for large-scale earthquake simulations. Further, hybrid phase-field fracture mechanics ([Ambati et al., 2015](#)) is implemented, which enables detailed analysis of crack initiation and propagation in materials. These types of simulations are treated at the other end of the complete simulation chain from the earthquake source to the structure assessment.

A distinguishing feature of PSD is its ability to handle large-scale earthquake simulations ( $\mathcal{O}(10^9)$ ), particularly in fault-to-site analysis scenarios. This capability, combined with the solver's parallel architecture and advanced material modeling, makes it particularly suitable for comprehensive seismic risk assessment studies. The solver exhibits excellent scalability on tens of thousands of MPI processes, enabling simulations with billions of unknowns on large scale supercomputers. This allows it to accurately capture the multiscale features of seismic wave propagation and consequences—from fault to local site response.

## Statement of Need

Seismic risk assessment require computational tools capable of simulating wave propagation across multiple spatial scales, from fault (kilometers away) to local site response (meters), while ensuring sufficient accuracy for earthquake engineering analyses. Existing commercial solutions often lack the computational scalability required for integrated regional to local scale earthquake simulations, while open-source alternatives typically address only specific aspects of the seismic simulation workflow.

Current computational challenges in earthquake simulation include: (1) the need for billions of degrees-of-freedom to capture realistic fault-to-site scenarios ([Hori et al., 2018](#)), ([Cui et al., 2013](#)) (2) integration of complex non-linear material behaviors and damage assessment for solids and structures, and (3) efficient mesh generation and partitioning for irregular geological

domains often constructed directly from digital elevation models. Tools like OpenSees (McKenna, 2011) excel in local site response analysis (soils and structures) based on the finite element method (FEM) and SPEC3D (Peter et al., 2011) or SEM3D (Touhami et al., 2022) address seismic wave propagation using the spectral element method. However, it is of interest to have an open-source integrated platform addressing the complete fault-to-site simulation workflow with HPC scalability.

PSD tries to fill this gap by providing a unified computational framework that combines earthquake source modeling, wave propagation simulation, and structural mechanics assessment within a single scalable FEM solver. PSD's integration of advanced meshing-partitioning capabilities (top-ii-vol), sophisticated material modeling (Mfront interface), and fracture mechanics positions it uniquely for comprehensive seismic risk assessment needs requiring both regional-scale wave propagation and local site response including structural analysis.

## PSD Features and Architecture

PSD provides a comprehensive suite of physics modules addressing diverse computational mechanics applications around earthquake simulations. It includes dedicated modules for linear elasticity, elastodynamics, fracture mechanics, soil dynamics<sup>1</sup>, and elasto-plasticity, making it suitable for applications ranging from static structural analysis to dynamic earthquake simulation and material damage assessment. The Mfront interface significantly enhances this versatility by enabling users to implement custom non-linear material models that can be integrated into any of these physics modules, extending PSD's applicability beyond the built-in constitutive laws.

PSD adopts a layered architecture that separates mathematical formulation from computational implementation while maintaining high performance through strategic integration with FreeFEM for finite element discretization, PETSc for scalable linear algebra, and Mfront for sophisticated material modeling. PSD follows a code generation approach where users specify problem configurations through command-line options, and the software automatically generates optimized code tailored to specific physics, dimensionality, and boundary conditions. This design enables computational efficiency while preserving flexibility for diverse solid mechanics applications across the available physics modules.

The parallel computing architecture in PSD employs domain decomposition strategies which enable distribute memory parallelization which are optimized for large-scale FEM simulation (Dolean et al., 2015). PSD has demonstrated scalability up to 24,000 cores and capability for handling problems with over 5 billion unknowns for earthquakes. The integration with the top-ii-vol meshing tool provides efficient on the fly mesh generation and partitioning specifically designed for earthquake simulation geometries, eliminating traditional bottlenecks associated with sequential meshing approaches.

Each of PSD's module undergoes comprehensive validation and verification testing to ensure numerical accuracy and reliability across its diverse physics modules. The validation framework includes cross-comparison with established numerical codes, comparison with experimental results, and verification against manufactured analytical solutions. Some of the validation results covering all physics modules are documented and publicly available at <https://mohd-afeef-badri.github.io/psd/validation>, providing users with confidence in the PSD's accuracy for their specific applications.

<sup>1</sup>The *soildynamics* module builds upon the elastodynamics module by incorporating specialized tools essential for earthquake modeling, such as paraxial (absorbing) boundary conditions, double-couple source mechanisms, point-cloud meshing-partitioning algorithm, etc.

## Example Workflow for Earthquake Simulation in PSD

The following workflow demonstrates PSD's `soildynamic` module through a fundamental large-scale earthquake simulation problem: seismic wave propagation in a three-dimensional elastic soil domain with absorbing boundaries and seismic excitations represented through double-couple point source. This example illustrates one of PSD's specialized physics modules among others, the aim here is to briefly illustrate PSD's key capabilities including automated distributed mesh generation (combined meshing-partitioning), advanced time integration, and sophisticated boundary condition handling.

**Mathematical Presentation:** PSD solves the elastodynamic wave equation using finite element discretization with Newmark- $\beta$  time integration<sup>2</sup>. The implementation incorporates paraxial absorbing boundaries (Modaresi & Benzenati, 1994) to prevent artificial wave reflections, essential for realistic earthquake simulations, and seismic source excitations with double-couple theory (Benz & Smith, 1987).

For a 3D domain  $\Omega \subset \mathbb{R}^3$  bounded by boundaries  $\partial\Omega \subset \mathbb{R}^3$  and with paraxial absorbing boundaries  $\partial\Omega_p \subset \partial\Omega$ , the finite element variational formulation solved in PSD reads:

Find  $\mathbf{u} \in \mathcal{U}$  such that  $\forall t \in [0, t_{\max}], \forall \mathbf{v} \in \mathcal{V}$ :

$$\begin{aligned} \int_{\Omega} \left( \frac{\rho}{\beta \Delta t^2} \mathbf{u} \cdot \mathbf{v} + \boldsymbol{\sigma}(\mathbf{u}) : \boldsymbol{\varepsilon}(\mathbf{v}) \right) + \int_{\partial\Omega_p} \frac{\rho\gamma}{\beta \Delta t} \mathbf{u} \cdot \mathbf{P} \cdot \mathbf{v} = \\ \int_{\Omega} \frac{\rho}{\beta} \left( \frac{1}{\Delta t^2} \mathbf{u}_{\text{old}} \cdot \mathbf{v} + \frac{1}{\Delta t} \dot{\mathbf{u}}_{\text{old}} \cdot \mathbf{v} + \left( \frac{1}{2} - \beta \right) \ddot{\mathbf{u}}_{\text{old}} \cdot \mathbf{v} \right) + \\ \int_{\partial\Omega_p} \left( \frac{\rho\gamma}{\beta \Delta t} \mathbf{u}_{\text{old}} \cdot \mathbf{P} \cdot \mathbf{v} + \left( \frac{\rho\gamma}{\beta} - \rho \right) \dot{\mathbf{u}}_{\text{old}} \cdot \mathbf{P} \cdot \mathbf{v} + \left( \frac{\rho\gamma \Delta t}{2\beta} - \rho \Delta t \right) \ddot{\mathbf{u}}_{\text{old}} \cdot \mathbf{P} \cdot \mathbf{v} \right). \end{aligned}$$

Here:

- $(\mathbf{u}, \mathbf{v}) : \Omega \rightarrow \mathbb{R}^3$  are the finite element trial (unknown displacement) and test functions, respectively, defined in finite element linear closed spaced  $(\mathcal{U}, \mathcal{V})$  defined in  $[H^1(\Omega)]^3$ . Additionally, at time  $t = 0$ ,  $\mathbf{u}$  must fulfill the initial conditions  $\mathbf{u} = \mathbf{u}_0$  and  $\dot{\mathbf{u}} = \dot{\mathbf{u}}_0$ . Since no Dirichlet boundary conditions are considered here,  $\mathcal{U}$  and  $\mathcal{V}$  coincide. In more general cases, fields in  $\mathcal{U}$  satisfy Dirichlet conditions, whereas fields in  $\mathcal{V}$  vanish on the corresponding boundaries.
- $(\mathbf{u}_{\text{old}}, \dot{\mathbf{u}}_{\text{old}}, \ddot{\mathbf{u}}_{\text{old}}) : \Omega \rightarrow \mathbb{R}^3$  represent respectively the displacement, velocity, and acceleration fields computed at previous time step and defined over  $\Omega$ ;
- $(\boldsymbol{\sigma}(\mathbf{u}), \boldsymbol{\varepsilon}(\mathbf{v})) : \Omega \rightarrow \mathbb{R}^{3 \times 3}$  represent the linear elastic Cauchy stress tensor and the small strain tensor, respectively, both rank-2 tensor fields;
- $(\rho, \gamma, \beta, t, t_{\max}, \Delta t) \in \mathbb{R}$  are scalar parameters corresponding to soil density ( $\rho$ ), Newmark- $\beta$  time discretization parameters ( $\gamma, \beta$ ), and time variables ( $t, t_{\max}, \Delta t$ );
- $\mathbf{P} : \partial\Omega_p \rightarrow \mathbb{R}^{3 \times 3}$  is a direction-dependent impedance tensor enforcing paraxial absorbing boundary conditions on the boundary  $\partial\Omega_p$ . It is defined as:

$$\mathbf{P} = c_p \mathbf{n} \otimes \mathbf{n} + c_s (\mathbf{I} - \mathbf{n} \otimes \mathbf{n}),$$

<sup>2</sup>PSD implements the generalized- $\alpha$  time discretization method (Chung & Hulbert, 1993), which encompasses several classical time integration schemes as special cases depending on the parameter selection: central difference, HHT (Hilber-Hughes-Taylor) (Hilber et al., 1977), and Newmark- $\beta$  methods.

115 where,  $\mathbf{n} : \partial\Omega_P \rightarrow \mathbb{R}^3$  is the outward unit normal vector on the boundary,  $\mathbf{I} \in \mathbb{R}^{3 \times 3}$  is  
116 the identity  $2^{nd}$ -order tensor, ( $c_p, c_s \in \mathbb{R}$ ) are scalar parameters corresponding to the  
117 P-wave and S-wave wave velocities in the soil.

118 Finally, seismic excitation is applied via a double-couple point source, where the seismic moment  
119 tensor  $\mathbf{M}$  is derived from standard source parameters (fault dip, rake, and strike).  $\mathbf{M}$  is a  
120 symmetric tensor representing the equivalent point forces that reproduce the elastic waves  
121 radiated by an earthquake, i.e., the second moment of the force distribution in the source  
122 region. This tensor is imposed through equivalent displacements (Dirichlet conditions) at four  
123 points north, south, east, and west of the source within  $\Omega$ . Formally, for  $\{\mathbf{x}_i\}_{i=0}^4 \in \Omega$ , the  
124 imposed displacements are  $\mathbf{u}(\mathbf{x}_i, t) = \mathbf{d}_i(t) = \mathbf{f}(\mathbf{M}, t)$ , where  $\mathbf{f}(\mathbf{M}, t)$  maps  $\mathbf{M}$  and its time  
125 dependence to displacement histories at each point, reproducing the seismic moment release  
126 and radiation pattern. For smaller-scale problems, excitation can alternatively be prescribed  
127 via time-dependent Dirichlet or Neumann (force) boundary conditions.

128 **Workflow:** The PSD workflow begins with automated code generation through the  
129 PSD\_PreProcess utility, which generates problem-specific finite element code based on user  
130 specifications. This approach ensures computational efficiency while maintaining flexibility for  
131 different problem configurations.

132 Sample preprocessing command:

```
133 PSD_PreProcess -problem soildynamics -dimension 3 -top2vol-meshing \  
134 -timediscretization newmark_beta -postprocess uav
```

135 Material parameters are then specified through ASCII configuration file, with typical values  
136 for soil properties including density and wave velocities corresponding to standard engineering  
137 geology classifications:

```
138 real rho = 1800.0 , // Density (kg/m³)  
139 cs = 2300.0 , // S-wave velocity (m/s)  
140 cp = 4000.0 ; // P-wave velocity (m/s)
```

141 Time discretization parameters follow established earthquake engineering practices, with time  
142 steps chosen to satisfy numerical stability requirements for wave propagation:

```
143 real tmax = 20.0 , // Total simulation time  
144 t = 0.001 , // Initial time  
145 dt = 0.001 ; // Time step  
146  
147 real gamma = 0.5 ,  
148 beta = (1./4.)*(gamma+0.5)^2 ;
```

149 The simulation is executed using the parallel solver with the specified number of MPI processes:

```
150 PSD_Solve -np 6144 Main.edp #6144 MPI-domains are used
```

151 Results such as those presented in Figure 1 can be obtained by launching PSD simulation.  
152 These results corresponds to seismic wave propagation for hypothetical earthquake. These  
153 simulations may then used for risk assessments of potential sites of interest for engineering.

## 154 Demonstration

155 Figure 1 presents a regional-scale earthquake simulation of the French Cadarache region  
156 performed with PSD, as detailed in (Badri et al., 2024). This simulation demonstrates PSD's  
157 capability for large-scale seismic wave propagation modeling, involving over one billion degrees  
158 of freedom distributed across 6144 MPI domains. The displacement fields shown at four time  
159 intervals illustrate wave propagation patterns characteristic of earthquake scenarios, with  
160 computational complexity approaching operational seismic hazard assessment requirements.

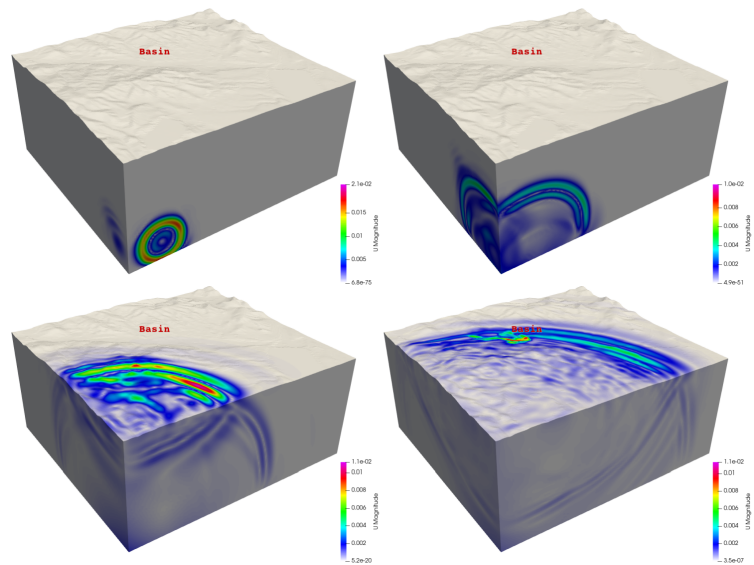


**Figure 1:** Regional-scale earthquake simulation of the French Cadarache region (50 km  $\times$  50 km) showing displacement magnitude at four time steps, using a 540-million-element mesh (10 m resolution),  $\Delta t = 10^{-3}$  s, and Newmark- $\beta$  parameters  $(\beta, \gamma) = (0.5, 0.25)$ .

Figure 2 demonstrates PSD's fracture mechanics capabilities through a quasi-static brittle fracture simulation within a perforated medium, as presented in (Badri et al., 2021). This simulation involves more than 64 million degrees of freedom solved across 1008 MPI domains on the French Joliot-Curie supercomputer, illustrating the software's capability for detailed damage assessment applications that complement regional-scale earthquake simulations.

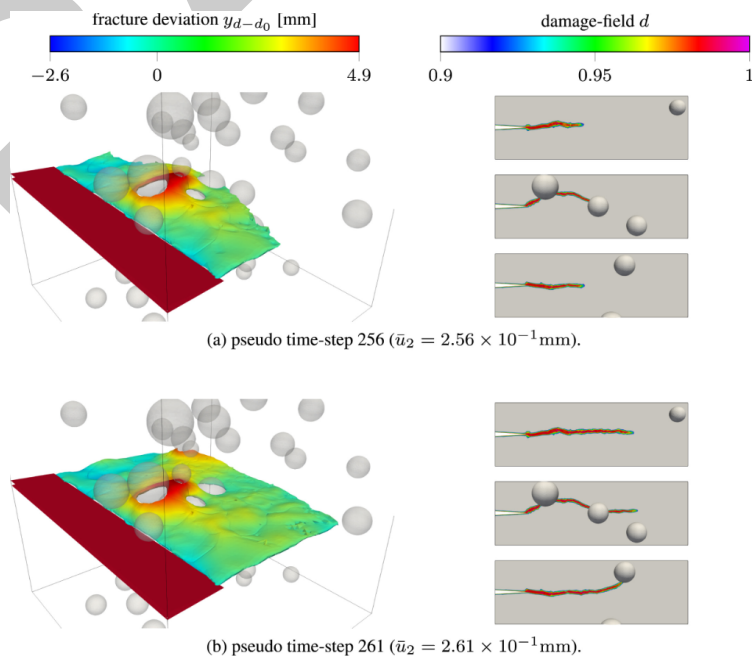


**Figure 2:** Crack propagation for a perforated medium, simulation performed with PSD.

These demonstrations represent significant computational achievements, with problem sizes nearing those required for operational seismic hazard and risk assessment. The simulation of the Cadarache region in France demonstrates PSD's applicability to real-world earthquake

169 engineering problems, while the fracture mechanics example illustrates the software's capability  
170 for detailed damage assessment applications.

171 Additional applications demonstrate PSD's versatility for advanced fracture mechanics re-  
172 search, including eikonal non-local gradient damage model implementations (Nogueira et al.,  
173 2023), (Nogueira et al., 2024), which further extend the software's capabilities for comprehensive  
174 structural analysis.

## 175 Documentation and Availability

176 PSD is distributed under the Apache License, Version 2.0, ensuring broad accessibility for research  
177 and educational applications. PSD's repository at <https://github.com/mohd-afeef-badri/psd>  
178 includes comprehensive documentation covering cross-platform installation procedures (based  
179 on Autotools), usage examples, and validation test cases. Continuous integration testing, via  
180 GitHub Actions, ensures software reliability across different computing environments, while the  
181 modular architecture facilitates community contributions and ongoing development.

## 182 Acknowledgements

183 This work is supported by the French Alternative Energies and Atomic Energy Commission  
184 (CEA) through the GEN2&3 program funding. The authors gratefully acknowledge TGCC,  
185 France, for providing access to the Joliot-Curie supercomputer under the GENDEN computing  
186 quota. This research was initially funded by the PTC HPCSEISM program at CEA during the  
187 2018–2021 period. G. Rastiello was also supported by the SEISM Institute (France).

188 The authors also acknowledge key contributors to the PSD solver: Dr. Breno Ribeiro Nogueira  
189 for his Ph.D. work on the fracture mechanics module via the MFront interface, Dr. Reine Fares  
190 for integrating Iwan non-linear soil behavior model via the Mfront interface, and Rania Saadi  
191 for enabling the parallel mesh adaptation kernel.

## 192 References

- 193 Ambati, M., Gerasimov, T., & De Lorenzis, L. (2015). A review on phase-field models of  
194 brittle fracture and a new fast hybrid formulation. *Computational Mechanics*, 55, 383–405.  
195 <https://doi.org/10.1007/s00466-014-1109-y>
- 196 Badri, M. A., Bourcier, C., & Foerster, E. (2024). Top-ii-vol: Massively parallel scalable  
197 meshing for seismic risk assessment of nuclear sites. *EPJ Web of Conferences*, 302, 05007.  
198 <https://doi.org/10.1051/epjconf/202430205007>
- 199 Badri, M. A., Rastiello, G., & Foerster, E. (2021). Preconditioning strategies for vectorial finite  
200 element linear systems arising from phase-field models for fracture mechanics. *Computer*  
201 *Methods in Applied Mechanics and Engineering*, 373, 113472. <https://doi.org/10.1016/j.cma.2020.113472>
- 203 Balay, S., Abhyankar, S., Adams, M., Brown, J., Brune, P., Buschelman, K., Dalcin, L.,  
204 Dener, A., Eijkhout, V., Gropp, W., & others. (2019). *PETSc users manual*. <https://doi.org/10.2172/1814627>
- 206 Benz, H. M., & Smith, R. B. (1987). Kinematic source modelling of normal-faulting earthquakes  
207 using the finite element method. *Geophysical Journal International*, 90(2), 305–325.  
208 <https://doi.org/10.1111/j.1365-246x.1987.tb00729.x>
- 209 Chung, J., & Hulbert, G. M. (1993). A time integration algorithm for structural dynamics with  
210 improved numerical dissipation: The generalized- $\alpha$  method. *Journal of Applied Mechanics*,  
211 60(2), 371–375. <https://doi.org/10.1115/1.2900803>



- 212 Cui, Y., Poyraz, E., Olsen, K. B., Zhou, J., Withers, K., Callaghan, S., Larkin, J., Guest,  
213 C., Choi, D., Chourasia, A., & others. (2013). Physics-based seismic hazard analysis on  
214 petascale heterogeneous supercomputers. *Proceedings of the International Conference on*  
215 *High Performance Computing, Networking, Storage and Analysis*, 1–12. <https://doi.org/10.1145/2503210.2503300>  
216
- 217 Dolean, V., Jolivet, P., & Nataf, F. (2015). *An introduction to domain decomposition*  
218 *methods: Algorithms, theory, and parallel implementation*. SIAM. <https://doi.org/10.1137/1.9781611974065>  
219
- 220 Hecht, F. (2012). New development in FreeFem++. *Journal of Numerical Mathematics*,  
221 20(3-4), 251–265. <https://doi.org/10.1515/jnum-2012-0013>
- 222 Helfer, T., Bleyer, J., Frondelius, T., Yashchuk, I., Nagel, T., & Naumov, D. (2020). The  
223 'MFrontGenericInterfaceSupport' project. *Journal of Open Source Software*, 5(48), 2003.  
224 <https://doi.org/10.21105/joss.02003>
- 225 Helfer, T., Michel, B., Proix, J.-M., Salvo, M., Sercombe, J., & Casella, M. (2015). Introducing  
226 the open-source mfront code generator: Application to mechanical behaviours and material  
227 knowledge management within the PLEIADES fuel element modelling platform. *Computers*  
228 *& Mathematics with Applications*, 70(5), 994–1023. <https://doi.org/10.1016/j.camwa.2015.06.027>  
229
- 230 Hilber, H. M., Hughes, T. J., & Taylor, R. L. (1977). Improved numerical dissipation for  
231 time integration algorithms in structural dynamics. *Earthquake Engineering & Structural*  
232 *Dynamics*, 5(3), 283–292. <https://doi.org/10.1002/eqe.4290050306>
- 233 Hori, M., Ichimura, T., Wijerathne, L., Ohtani, H., Chen, J., Fujita, K., & Motoyama, H. (2018).  
234 Application of high performance computing to earthquake hazard and disaster estimation in  
235 urban area. *Frontiers in Built Environment*, 4, 1. <https://doi.org/10.3389/fbuil.2018.00001>
- 236 McKenna, F. (2011). OpenSees: A framework for earthquake engineering simulation. *Comput-*  
237 *ing in Science & Engineering*, 13(4), 58–66. <https://doi.org/10.1109/MCSE.2011.66>
- 238 Modaressi, H., & Benzenati, I. (1994). Paraxial approximation for poroelastic  
239 media. *Soil Dynamics and Earthquake Engineering*, 13(2), 117–129. [https://doi.org/10.1016/0267-7261\(94\)90004-3](https://doi.org/10.1016/0267-7261(94)90004-3)  
240
- 241 Nogueira, B. R., Rastiello, G., Giry, C., Gatuingt, F., & Callari, C. (2024). Eikonal gradient-  
242 enhanced regularization of anisotropic second-order tensorial continuum damage models  
243 for quasi-brittle materials. *Computer Methods in Applied Mechanics and Engineering*, 429,  
244 117100. <https://doi.org/10.1016/j.cma.2024.117100>
- 245 Nogueira, R. B., Rastiello, G., Giry, C., Gatuingt, F., & Callari, C. (2023). Numerical  
246 simulations of concrete specimens with the gradient-enhanced Eikonal non-local damage  
247 model. *Academic Journal of Civil Engineering*, 41(1). <https://doi.org/10.26168/ajce.41.1.30>  
248
- 249 Peter, D., Komatitsch, D., Luo, Y., Martin, R., Le Goff, N., Casarotti, E., Le Loher, P.,  
250 Magnoni, F., Liu, Q., Blitz, C., Nissen-Meyer, T., Basini, P., & Tromp, J. (2011). Forward  
251 and adjoint simulations of seismic wave propagation on fully unstructured hexahedral  
252 meshes. *Geophysical Journal International*, 186(2), 721–739. <https://doi.org/10.1111/j.1365-246X.2011.05044.x>  
253
- 254 Touhami, S., Gatti, F., Lopez-Caballero, F., Cottureau, R., Abreu Corrêa, L. de, Aubry, L.,  
255 & Clouteau, D. (2022). SEM3D: A 3D high-fidelity numerical earthquake simulator for  
256 broadband (0–10 Hz) seismic response prediction at a regional scale. *Geosciences*, 12(3),  
257 112. <https://doi.org/10.3390/geosciences12030112>